Fuel 381 (2025) 133253

Contents lists available at ScienceDirect

Fuel

journal homepage: www.elsevier.com/locate/fuel

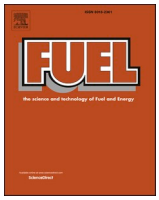

Full Length Article

Combustion of NH_3/DME and NH_3/DME/NO mixtures

A. Ruiz-Gutiérrez, P. Rebollo, M.U. Alzueta *

Aragón Institute of Engineering Research (I3A), Department of Chemical and Environmental Engineering, University of Zaragoza, 50018 Zaragoza, Spain

ARTICLE INFO

Keywords:
NH_3
DME
NH_3/DME mixtures
NO
Kinetic modelling

ABSTRACT

The objective of this work is to study the oxidation of ammonia and dimethyl ether mixtures (NH_3/DME) both in the absence and the presence of monoxide of nitrogen (NO). For this purpose, laboratory experiments have been conducted in a quartz flow reactor setup in the 875–1425 K temperature range at atmospheric pressure, modifying the oxygen excess ratio (λ), and the NH_3/DME mixture ratio with and without NO. The experimental results have been simulated with a literature-based kinetic mechanism. The results show that the presence of DME and an oxygen excess ratio affect the conversion of NH_3, shifting its oxidation to lower temperatures, which decrease as the DME concentration in the mixture and λ increase. Interactions between ammonia and DME seem to be important under the studied conditions, presumably involving the formation and thermal decomposition of methyl nitrite (CH_3ONO). These interactions affect the oxidation of ammonia at low temperatures, consume and produce NO, which would determine the final NO emission. When there is NO in the NH_3/DME mixtures, NO is reduced up to 60 %, also favouring the oxidation of ammonia, but with an almost imperceptible effect of NO in the case of DME. The addition of different concentrations of DME also affects the oxidation behaviour of ammonia in NH_3/DME/NO mixtures. In general, the conversion of both NH_3 and DME is highly determined by the concentration of OH radicals, although thermal decomposition is also relevant for DME.

1. Introduction

Currently, hydrocarbon fuels [1] are the most used energy sources. If these fuels have a fossil origin, their use constitutes one of the main causes of climate change through the emission of CO_2, an important greenhouse gas. To mitigate climate change, many countries have designed zero-emission plans [2] that aim to both reduce CO_2 emissions and develop cleaner technologies. Furthermore, the objective is that 66 % of the energy used by 2050 [3] comes from a clean energy source. To achieve this goal, it is possible to use different renewable energies such as solar, geothermal, wind, or biofuel, among others.

One interesting alternative may rely on the use of ammonia, either as a fuel or as an energy carrier. Ammonia can be produced either from fossil fuels, biomass or renewable energies. Renewable energies such as wind or photovoltaic can be profitable if the excess energy can be utilized [4]. Also, ammonia is an excellent hydrogen storage medium. NH_3 has a lower cost per unit of stored energy (0.54 $) than hydrogen itself (14.95 $) [5]. In addition, there is currently a remarkable infrastructure for the handling and transport of NH_3, due to the advanced development of the ammonia industry and the extended use of this chemical, with a transportation capacity of more than 100 million tons per year [6,7]. This means that when ammonia is used as a fuel the need for investments is low. So far, there is already evidence of efficiently operating systems based on ammonia combustion. In Japan, the Fukushima Renewable Energy Institute of the National Institute of Advanced Industrial Science and Technology has reported success in running a microturbine using pure ammonia, generating up to 42 kW of power [8], although it has been necessary to implement a selective catalytic reduction (SCR) system to reduce NO_x emissions to comply with regulatory levels. Also, a series of tests have been conducted at the Mizushima plant, where NH_3 has been added to coal combustion. The presence of ammonia, with a mixture percentage between 0.6–0.8 %, did not affect the plant performance. Consequently, the addition of ammonia caused a decrease in the carbon dioxide emitted [9]. NH_3 has also been used directly in other systems, such as combustion engines [10,11] or fuel cells [12], indicating a promising use of ammonia as a combustible.

While the use of ammonia seems plausible in the near future, it also has some disadvantages. As a non-carbon compound, it has a low calorific value, low flame velocity, poor flammability and a high self-ignition temperature [13]. In order to overcome these problems, one possibility to facilitate the ignition of ammonia is based on mixing it with other fuels, such as hydrogen or hydrocarbons. Currently, the most studied

* Corresponding author.
E-mail address: uxue@unizar.es (M.U. Alzueta).

https://doi.org/10.1016/j.fuel.2024.133253
Received 2 May 2024; Received in revised form 18 September 2024; Accepted 19 September 2024
Available online 4 October 2024

compounds to be mixed with ammonia for its combustion are CH_4 and H_2. Dai et al. [14] showed that the presence of methane in the combustion of NH_3 modifies the ignition delay time, despite the fact that the presence of CH_4 causes CO_2 emissions proportional to the percentage of methane in the mixture [15,16]. H_2 is of great interest due to the absence of carbon in its composition. Consequently, many studies have been carried out to evaluate the performance of NH_3-H_2 mixtures [17–22], investigating their combustion properties, as well as their NO emissions. Nowadays, the mixing of NH_3 with oxygenated organic compounds is being considered, because oxygenates that contain one or more oxygen atoms in their molecular structure have been used as fuel additives since the 1970 s. The addition of these chemicals, even in small quantities, has been shown to reduce soot emissions from diesel fuels, increase the anti-knock power of gasolines and optimise combustion [23,24]. Some of the most studied oxygenated compounds are dimethyl ether (DME) [25–27], diethyl ether (DEE) [28–30], dimethoxymethane (DMM) [31] or methanol [32,33].

One of the most promising additives to be mixed with ammonia is DME. It has great potential as a fuel for automotive vehicles and for power generation [34] due to its well-developed storage and production technology, with a global production of around 150,000 tons per year. Moreover, this compound can be synthesised from renewable energies (biomass, waste or agricultural products) [35,36]. The higher cetane number of DME compared to diesel fuel [37], its good miscibility with many hydrocarbons [38] and the fact that it can reduce the auto-ignition of NH_3 are also worth mentioning. Additionally, DME has lower soot emissions than conventional fuels, due to the absence of C–C bonds in DME [39]. It also shows minimum NO_x emissions due to its specific heat capacity and low heating value [39], which also imply a low adiabatic flame temperature. When burning DME, Lee et al. [40], reported a reduction of up to 40 % in NO_x emissions with high exhaust gas ratios without visible smoke or a decrease in engine efficiency.

Experimental studies on the conversion of NH_3/DME mixtures include those performed in jet stirred reactors [6,41,42], a homogenous batch reactor [43], a spherical combustion chamber [25], rapid compression machines (RCM) [44–46], a plug flow reactor [47] and a constant volume spherical reactor (CVSR) [45]. The main results drawn from these studies indicate that the presence of DME has a significant effect on the performance of ammonia combustion.

DME has been reported to promote NH_3 oxidation due to the lower auto-ignition temperature of dimethyl ether [6,41]. Also, the addition of DME to NH_3 increases laminar burning velocities, due to the increase in the radical pool produced by DME and the decrease in the adiabatic flame temperature [41,45,48]. One of the important reactions for the conversion of the NH_3/DME mixture is (r1), which is responsible for the increase in the concentration of O and OH radicals. The radical OH is especially crucial for the initial oxidation of both fuels, except under pyrolysis conditions, where the thermal decomposition of DME is dominant, as will be seen later. Zhu et al. [6] reached similar conclusions by adding $CH_3OCH_2O_2$, one of the main intermediate compounds of DME conversion, to NH_3. The addition of DME to the NH_3/DME mixture also results in a lower emission of NO [26,43] compared to the combustion of net NH_3 despite the fact that once NH_2 radicals are formed from NH_3, the NH_2-NO interaction, specifically reactions (r2) to (r4), plays an important role in the reduction of NO [45] under conditions similar to those of the Thermal NO_x process [49].

$$O_2+H \rightleftharpoons O+OH \quad \text{(r1)}$$

The reduction of NO is not constant at all temperatures, but a minimum is reached, as is the case with the Selective Non-Catalytic Reduction process of NO (SNCR). Furthermore, the sensitising effect of NO during the combustion of fuels [e.g. 34] is well known, while the NH_3/NO ratio has been reported to have little effect on NO reduction [49–51].

$$NH_3+OH \rightleftharpoons NH_2+H_2O \quad \text{(r2)}$$

$$NH_2+NO \rightleftharpoons N_2+H_2O \quad \text{(r3)}$$

$$NH_2+NO \rightleftharpoons NNH+OH \quad \text{(r4)}$$

On the other hand, DME and NO can interact as well. Their interactions under oxidising conditions have also been studied previously [52]. Alzueta et al [52] have highlighted the interactions between CH_3 radicals formed from DME and NO under fuel lean conditions. Moreover, DME oxidation occurs at lower temperatures in the presence of NO (200 K less). This is not the case under stoichiometric or fuel-rich conditions, where DME behaviour is not modified by the presence of NO.

The effect of DME on NH_3/DME mixtures seems to be less important at high pressures, where an ignition delay time similar to that at atmospheric pressure is achieved [46]. The consumption of 100 % of the DME is reached before 20 % of the NH_3 is consumed, and something similar occurs with DME-CH_4 mixtures [53]. In the presence of NO, this species competes with DME and NH_3 to consume OH radicals, the main promoters of ammonia oxidation. Murakami et al. [47] have also shown that both DME and the CH_2O formed from DME have priority in O_2 consumption at low temperatures, between 800–1000 K, compared to NH_3. Ammonia oxidation also takes place within this temperature range and in the presence of DME, producing mainly NO and N_2O [47]. These latter species contribute to the generation of active radicals such as OH and CH_3O.

To our knowledge, the addition of NO to the NH_3/DME mixture has not been studied so far. Therefore, the present work is the first study to provide results on the NH_3/DME/NO mixture conversion and species profiles of the different products formed. Also, to our knowledge, there is no report of results on pyrolysis conditions for the considered mixtures, and these experiments will help to model development as well as to reflect on what can happen in the fuel-rich zones near the burner region. Additionally, the present study also extends the temperature range of previous works dealing with NH_3/DME mixtures to higher temperatures than those reported in the existing literature. In this context, this work aims to increase the database of NH_3/DME and NH_3/DME/NO mixtures with novel conditions and to determine the chemical reactions that take place during the oxidation of the mixtures.

2. Experimental methodology

The experiments have been carried out using a quartz flow reactor setup. The reactor has the internal dimensions of 8.7 mm in diameter and 200 mm in length and is placed within an electrical heated oven. Isothermal conditions have been achieved at ± 5 K. Temperature has been measured using a type-K fine-wire thermocouple. The temperature profile for the 20 cm length of the reactor is shown in Figure S1.1 of Supplementary Material S1. Flow rates have been set using mass flow controllers and confirmed using a series of volumetric flow meters. A total nominal gas flow rate of 1000 mL·min^{-1} (STP) has been constant throughout the experiments, which results in a gas residence time of 190 ms at 1000 K, and is calculated as a function of temperature and pressure following equation (1). Every gas (NH_3, O_2, DME, all diluted in argon and Ar used as bath gas to reach the total flow rate) has been taken from gas cylinders and fed to the reactor by individual injectors. Moreover, the main gas flow (Ar in all the experiments) was preheated in the reactor prior to its mixing with the rest of the gasses. The gas residence time has been calculated as a function of the reactor volume and the gas flow rate, and therefore varies with the temperature in the reactor. A more detailed description of the experimental setup and procedure can be found for instance in [54] and the schematic of the setup can be found in Figure S2.1 of Supplementary Material S2.

$$t_r = \frac{V_{reaction}}{Q_t(P_{ST}, T_{ST})} = \frac{192.097 \cdot P_{sr}}{Q_{t,N} \cdot T_{sr}} \quad (1)$$

where tr is the residence time (s), P_{sr} is the reactor pressure (mbar), T_{sr} is

the reactor temperature (K), and Q_t (P_{sr},T_{sr}) is the total reactant gas flow rate at the reactors pressure and temperature (ml/min).

An Agilent 490 Micro GC gas chromatograph equipped with TCD and FID detectors has been used to measure DME, CO, CO_2, CH_4, C_2H_6, C_2H_4, C_2H_2, NH_3, N_2O, H_2, N_2, O_2 and HCN. The error has been calculated according to the standard deviation, where the error does not depend on the temperature in the interval considered. It is an estimation of the experimental Micro GC error associated with the oxidation of NH_3 and DME. The largest uncertainty associated with the measurements for each temperature is ± 10 ppm. In addition, the outlet gas stream has been also analysed by an Advance Optima AO2020 series continuous gas analyser that measures the concentration of NO. The NO analyser has a measurement uncertainty of 1 %, but not less than 10 ppm. NO_2 concentrations are negligible in all the conditions studied.

The experimental parameters modified in the different experiments are: temperature, O_2 excess ratio (λ) and NH_3/DME ratio. Experimental conditions for the different experimental Sets are shown in Table 1.

The O_2 excess ratio, λ, equation (2) is defined as the ratio between the initial oxygen concentration fed in the experiment divided by the stoichiometric oxygen and calculated according to (r5) and (r6) reactions.

$$\lambda = \frac{O_{2fed}}{O_{2stoichoimetric}} \quad (2)$$

$$NH_3 + 0.75\ O_2 \rightarrow 0.5\ N_2 + 1.5\ H_2O \quad (r5)$$

$$CH_3OCH_3 + 3\ O_2 \rightarrow 2\ CO_2 + 3\ H_2O \quad (r6)$$

Experiments 1 to 12 correspond to the NH_3/DME mixture. Sets 13 to 23 correspond to the NH_3/DME/NO mixture. Pyrolysis experiments at different NH_3/DME ratio concentrations have been performed both in the absence and presence of NO (Sets 1, 2 and 13, 14, respectively). For the study of the oxygen excess ratio, nominal concentrations of 1000 ppm NH_3 and DME have been set (Sets 3–6) and the oxygen concentration has been modified in a range from 0 to 7452 ppm, which corresponds to λ values between 0 and 2. For the mixture containing NO, this compound also has an initial nominal concentration of 1000 ppm (Sets 15–17). To analyse the impact of the NH_3/DME mixing ratio, experiments 6–12 show the variation of the NH_3/DME ratio between 0.5 and 10 in the absence of NO and Sets 18–23 between 0.5 and 10 in the presence of NO.

Table 1
Experimental conditions. Balance is achieved with Ar. Concentrations are expressed in ppm.

Set	NH_3 (ppm)	DME (ppm)	O_2 (ppm)	NO (ppm)	NH_3/DME	λ	t_r (s)
1	913	977	0	0	0.93	0	190/T(K)
2	927	1943	0	0	0.48	0	190/T(K)
3	924	934	1859	0	0.99	0.53	191/T(K)
4	960	949	3218	0	1.01	0.90	191/T(K)
5	923	943	3855	0	0.98	1.09	190/T(K)
5R	924	934	3700	0	1.06	1.00	190/T(K)
6	938	946	7452	0	0.99	2.10	191/T(K)
7	1017	1936	3370	0	0.53	0.51	190/T(K)
8	927	1916	6533	0	0.48	1.01	190/T(K)
9	1066	2007	13,427	0	0.53	1.97	190/T(K)
10	1023	107	650	0	9.56	0.60	190/T(K)
11	1053	98	927	0	10.74	0.90	190/T(K)
12	1023	103	2138	0	9.93	1.98	190/T(K)
13	1041	998	0	1048	1.04	0	190/T(K)
14	1035	2008	0	1044	0.52	0	190/T(K)
15	1040	1027	1889	1023	1.01	0.50	189/T(K)
16	1012	997	3729	1030	1.02	0.99	189/T(K)
16R	1029	1012	3695	1016	1.02	0.99	190/T(K)
17	993	1000	7354	1030	0.99	1.96	189/T(K)
18	1024	2040	3317	1036	0.50	0.48	190/T(K)
19	997	2023	6678	992	0.49	0.98	189/T(K)
20	954	2008	13,320	998	0.48	1.98	189/T(K)
21	986	103	534	1023	9.57	0.51	190/T(K)
22	1021	103	1038	1020	9.91	0.98	189/T(K)
23	1038	109	2033	1013	9.52	1.89	190/T(K)

3. Chemical kinetic

Calculations have been performed using the mechanism of Glarborg et al. [55] as a basis. There are some minor updates for NH_3 [56], CH_3CN [57] and NH_3-NO [49] subsets, as explained by Alzueta et al. [58]. In turn, reactions of the DME subset, taken from the mechanism proposed by Marrodán et al. [23], have been added. The thermodynamic parameters used have been taken from the works indicated above. The kinetic model used includes a total of 142 species and 895 reactions. The simulations have been carried out using the Chemkin-Pro 2023 software [59] with the Pug Flow Reactor (PFR) module.

4. Results and discussion

4.1. Conversion of NH_3/DME mixtures

Fig. 1 shows the results of NH_3, DME and CO as a function of temperature under pyrolysis conditions (λ = 0) for two different NH_3/DME mixture ratios of 1 and 0.5. Hereinafter, *s*ymbols represent experimental results and lines correspond to model calculations. It is observed that without oxygen (Sets 1–2 of Table 1), the total decomposition of DME occurs at the same temperature (approximately 1100 K). This means that interactions of DME with ammonia in the absence of oxygen are not altered for different proportions of DME in the mixture. In turn, the decomposition of DME generates mostly CO in the absence of O_2. Regarding NH_3, there is a slightly higher conversion with an increased concentration of DME. This is attributed to the fact that the decomposition of DME occurs at a lower temperature than that of NH_3, which generates a radical pool and causes ammonia to react at a slightly lower temperature.

Fig. 2 shows the concentration profiles of NH_3, DME and NO, and Fig. 3 the concentration of the main products: N_2 and H_2, as a function of temperature for different stoichiometries ranging from pyrolysis to fuel lean conditions.NH_3 conversion starts at a lower temperature as the stoichiometric conditions become fuel leaner. Both DME and NH_3 show this behaviour, although the two compounds are seen to react independently at different temperature intervals, with DME conversion occurring at comparatively lower temperatures. It is observed that increasing the initial O_2 concentration leads to a faster oxidation of ammonia. This does not occur with DME, and no noticeable influence of oxygen concentration is found on DME conversion. DME is fully converted before 10 % of the NH_3 has reacted. The mechanism fits the DME profile very well, while the calculated ammonia conversion is sharper than observed experimentally.

A small amount of NO is formed during NH_3-DME oxidation, and the NO concentration increases with temperature. For the mixture proposed in Fig. 2 (NH_3/DME=1), the highest NO concentration (around 60 ppm) occurs under oxidizing conditions (λ = 2) and at the highest temperature (1425 K). NO shows two maximum concentration peaks. The first NO maximum is generated at the beginning of the NH_3 oxidation, as shown in Fig. 2. Then, the NO concentration decreases coinciding with the highest slope of the ammonia profile, but also with the presence of a high concentration of hydrocarbon radicals coming from DME, as will be discussed later. At the highest temperatures studied, the maximum NO concentrations are reached when both DME and NH_3 are fully converted. The kinetic model predicts higher NO emissions than those experimentally observed, as seen in Fig. 2c, even though the main trends are kept. At present, we don't know the exact reason for the discrepancies, but they may be due to the occurrence of reactions between NH_3-DME that the model does not properly take into account.

It is also interesting to note the two different temperature ranges for each fuel conversion, with DME being completely oxidised for the most

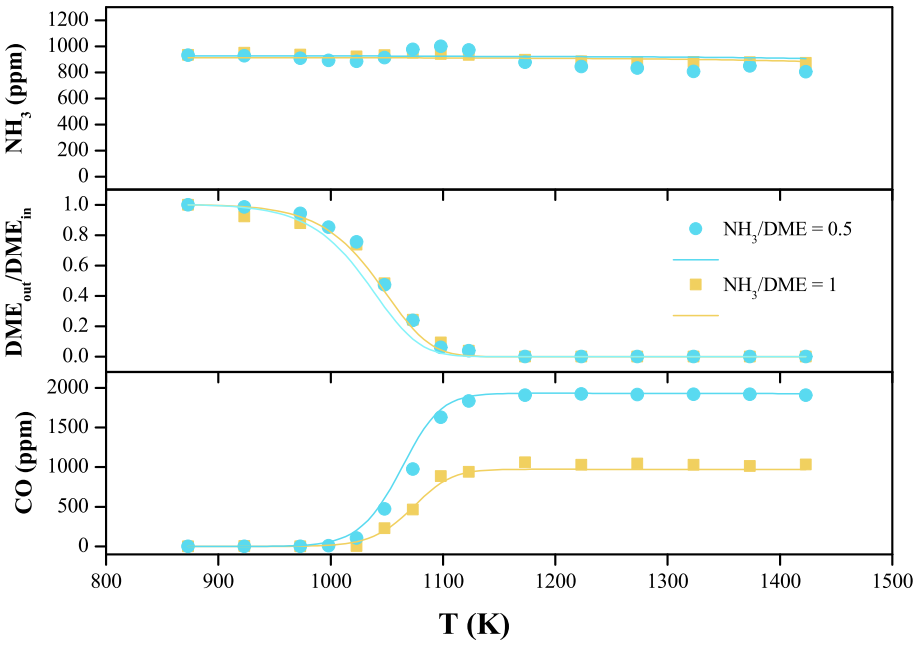

Fig. 1. NH_3, DME (normalised) and CO concentration as a function of temperature during the conversion of NH_3 for two different NH_3/DME mixture ratios. Sets 1 and 2 of Table 1.

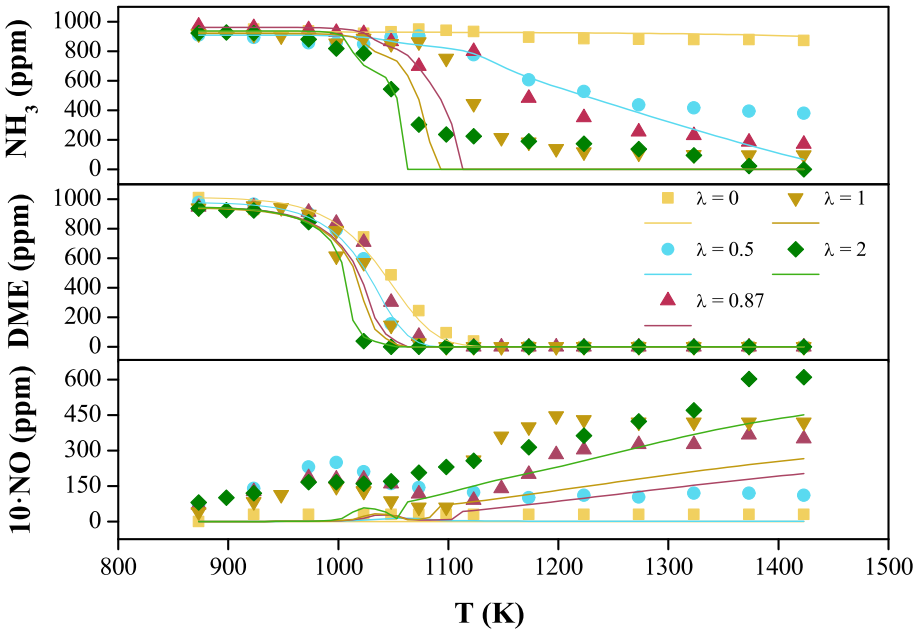

Fig. 2. NH_3, DME and NO concentrations as a function of temperature for different λ. Sets 1, 3–6 of Table 1. Experimental NO concentrations are multiplied by a factor of 10.

favourable case (Set 6) around 1050 K, while NH_3 is not completely oxidised even under pyrolysis conditions and at $\lambda \leq 0.87$. DME conversion is slightly favoured by increasing λ, even though the effect of this variable effect is much smaller than that observed for ammonia. This is because whereas the conversion of NH_3 is mostly initiated by reaction (r2): $NH_3+OH \rightleftharpoons NH_2+H_2O$, the initiation of DME conversion is thermal decomposition, which acts rapidly to feed the radical pool. Thus, there is no obvious evidence of direct interactions between NH_3 and DME under the studied conditions, although they may potentially happen.

The main products of ammonia conversion are N_2 and H_2, as shown in Fig. 3. Increasing the temperature results in an increase in nitrogen as a product for any λ, with the higher N_2 concentrations obtained in the fuel lean conditions, which are related to a higher conversion of ammonia. With respect to hydrogen, this species exhibits different behaviours as a function of temperature and the excess oxygen ratio. While a monotonic increase of H_2 as a function of temperature is seen under pyrolysis conditions, a maximum in H_2 concentration is found for the rest of λ, which diminishes as the stoichiometry becomes fuel leaner.

Fig. 4 shows as an example the concentrations of all species measured for stoichiometric conditions and a NH_3/DME ratio of 1. Other examples of the measured compounds are included in Supplementary Material S3 (Figures S3. 1–3).

In order to evaluate the quality of the experiments and to evidence if the main species produced during the conversion of the mixtures mainly

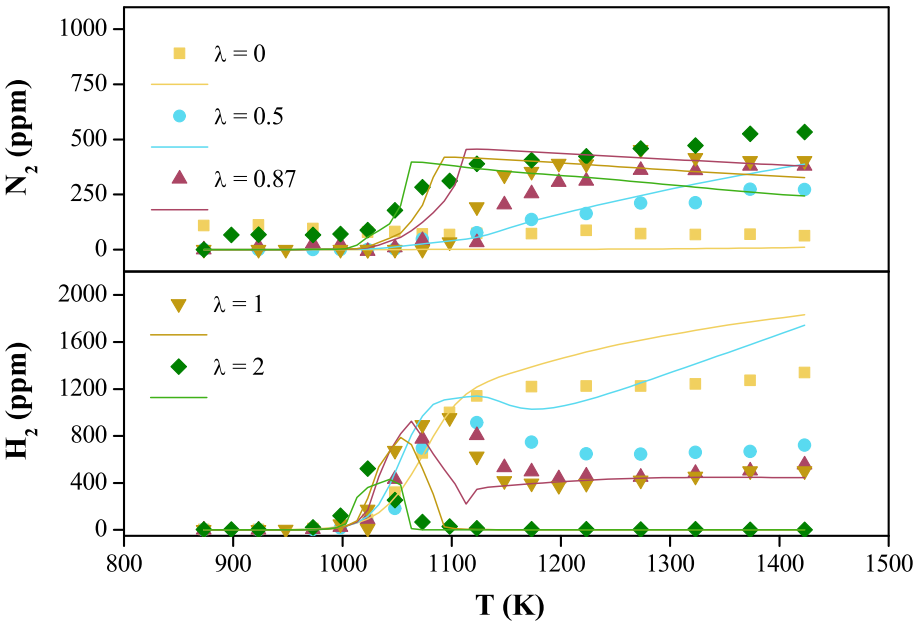

Fig. 3. N_2 and H_2 concentrations as a function of temperature for different λ. Sets 1, 3–6 of Table 1.

correspond with those experimentally determined, mass balances have been carried out for carbon and nitrogen atoms for four of the experiments performed and are shown in Fig. 5 as an example (similar results are obtained for all the experiments). The species included in the balances are those measured experimentally: CO, CO_2, CH_4, C_2H_6, C_2H_4, C_2H_2, NH_3, N_2O, H_2, N_2, O_2, HCN and NO. Simulations are also included as lines in Fig. 5 considering the same species as those measured in the experiments. In the case of formaldehyde, a species that may be present

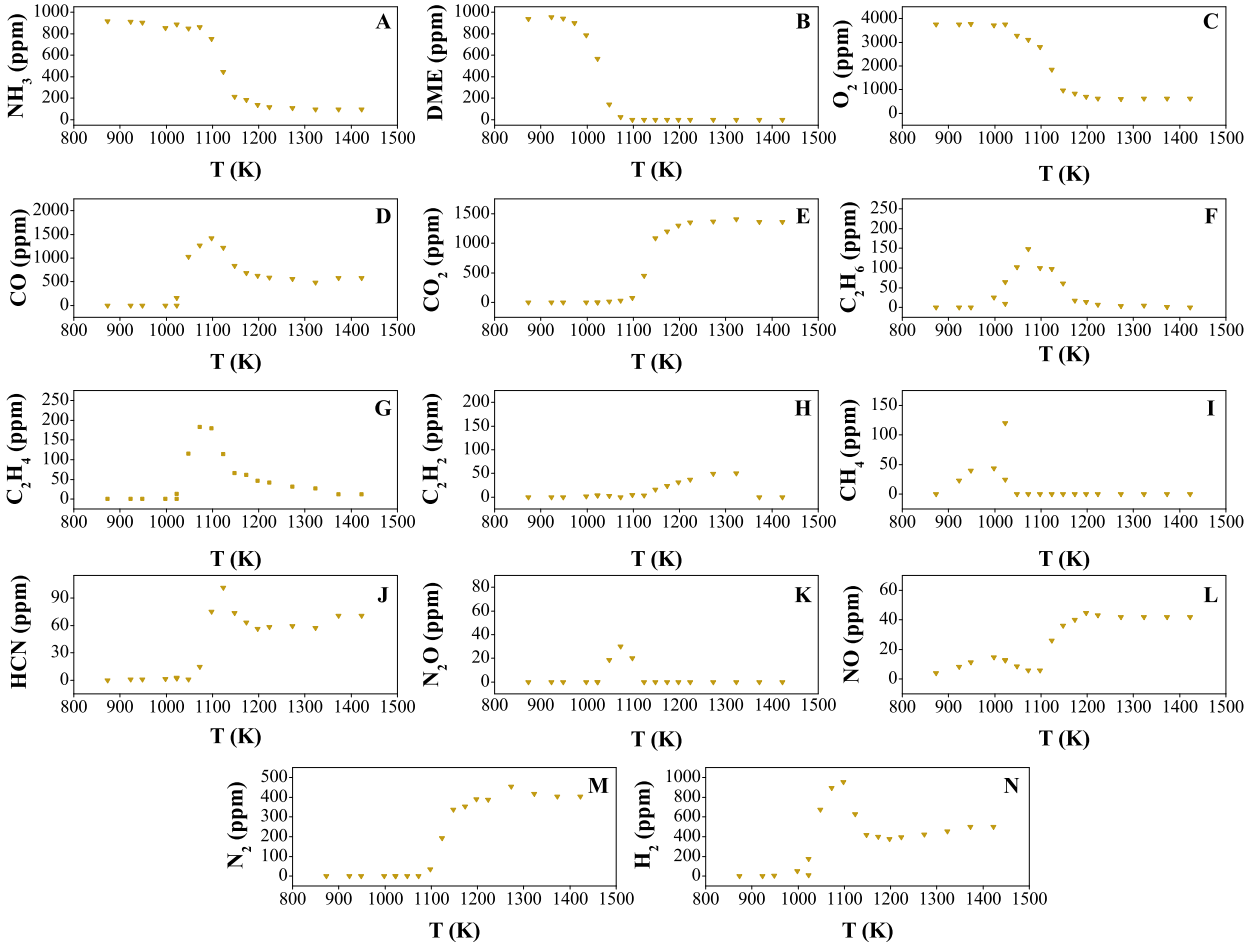

Fig. 4. Concentrations of the different species measured for the conditions of Set 5 of Table 1.

as a product in the current experiments, we can say that it is a challenging compound to be measured with the GC, since its signal coincides with that of methanol. For this reason, together with the additional difficulty of calibrating CH_2O, we have not measured this compound in the present experiments, and have set the calculated concentration of formaldehyde to be added to the mass balance (both experimental and calculated) since the model predicts the generation of formaldehyde in significant concentrations at low temperatures.

In general, mass balances for C and N close between 90 and 110 %, which indicates that the compounds identified in the experiments correspond to the C and N added to the reactor. The highest differences in the balances have been observed in the temperature ranges with the highest conversion of DME and NH_3, which means that additional intermediate species may be formed in that temperature zone. Figures S4.1 to S4.11 show additional examples of mass balances, which are included in Supplementary Material S4.

The impact of varying the NH_3/DME ratio has been evaluated by performing experiments in which the concentration of ammonia has been kept at a nominal concentration of 1000 ppm and the DME concentration has been varied between nominal concentrations of 2000 and 100 ppm (Sets 5, 8 and 11 respectively) all of them at $\lambda \approx 1$. The results of NH_3, DME and NO are shown in Fig. 6 as a function of temperature. The rest of the species measured under the conditions of Fig. 6 are included in Supplementary Material S5, Figures S5.1 to S5.11.

Varying the NH_3/DME ratio highly influences ammonia oxidation. Comparing the results of the ratio with less DME (NH_3/DME=10) and the ratio with more DME (NH_3/DME=0.5), the NH_3 profiles differ by about 200 K. Similarly, with the above variation of the NH_3/DME ratio, the complete oxidation of DME occurs with a difference of around 100 K. The mechanism reproduces fairly well the experimental observations. NO concentration is very low in the experiments at any temperature while it is overpredicted by the model. There is a maximum concentration of NO at low temperatures, as shown by calculations. Even though it is not shown, the variation of oxygen stoichiometry for the different NH_3/DME ratios has a similar effect to that seen for the ratio NH_3/DME=1.

The results of Fig. 6 show that NH_3 profile shows a behaviour similar to that of the NTC (negative temperature coefficient) behaviour reported in the literature for the low temperature oxidation regime of oxygenated organic compounds [6]. $NH_3+OH \rightleftharpoons NH_2+H_2O$ (r2) is the reaction that causes the highest ammonia consumption under all reaction conditions. Calculations indicate that the reaction $NH_2+HO_2 \rightleftharpoons NH_3+O_2$ (r7) is important under the conditions of Fig. 6 and responsible for the "NTC-NH_3" behaviour, bringing the concentration of NH_3 back to the initial values. For the NH_3/DME ratio of 1 under stoichiometric conditions at 1050 K, HO_2 is produced via $CH_2OH+O_2 \rightleftharpoons HCO+HO_2$ (r8) and $HCO+O_2 \rightleftharpoons CO+HO_2$ (r9), with CH_2O and HCO as intermediate products of the DME conversion.

The sensitivity analysis carried out for HO_2 (Figure S6.1 of the Supplementary Material) under these conditions shows that the HO_2 concentration is the most sensitive to the reactions: $HCO(+M) \rightleftharpoons H+CO(+M)$ (r10), $NH_2+NO \rightleftharpoons NNH+OH$ (r4) and $H+O_2 \rightleftharpoons O+OH$ (r1). The formation of HCO (r10) will promote the formation of HO_2, while the higher consumption of NO by the NH_2 radical (r4) favours a higher concentration of HO_2. According to the model, the formed HO_2 reacts quickly through reactions $NO+HO_2 \rightleftharpoons NO_2+OH$ (r11) and $NH_2+HO_2 \rightleftharpoons H_2NO+OH$ (r12). Since no NO_2 has been detected experimentally, it is conceivable for the conversion of NH_2 into H_2NO to be comparatively significant, as pointed out by Glarborg et al. [55]. In any case, it can be confirmed that the increase of the DME concentration in the mixture causes the NH_3 consumption to increase. For the case under study, this occurs at around 1000 K.

Fig. 7 shows the reaction pathways for the conversion of NH_3/DME when 10 % of ammonia has been consumed for the different excess oxygen ratios studied. Under all conditions, NH_3 oxidation starts with $NH_3+OH \rightleftharpoons NH_2+H_2O$ (r2). Subsequently, different behaviours are observed for $\lambda = 0.5$ compared to the stoichiometric and fuel lean conditions. As detailed below, the main reaction pathways for the conversion of NH_3/DME mixtures are:

(1) $NH_3 \rightarrow NH_2 \rightarrow N_2$.
(2) $NH_3 \rightarrow NH_2 \rightarrow H_2NO \rightarrow HNO \rightarrow NO \rightarrow NNH \rightarrow N_2$.
(3) $NH_3 \rightarrow NH_2 \rightarrow H_2NO \rightarrow HNO \rightarrow NO \rightarrow N_2$.

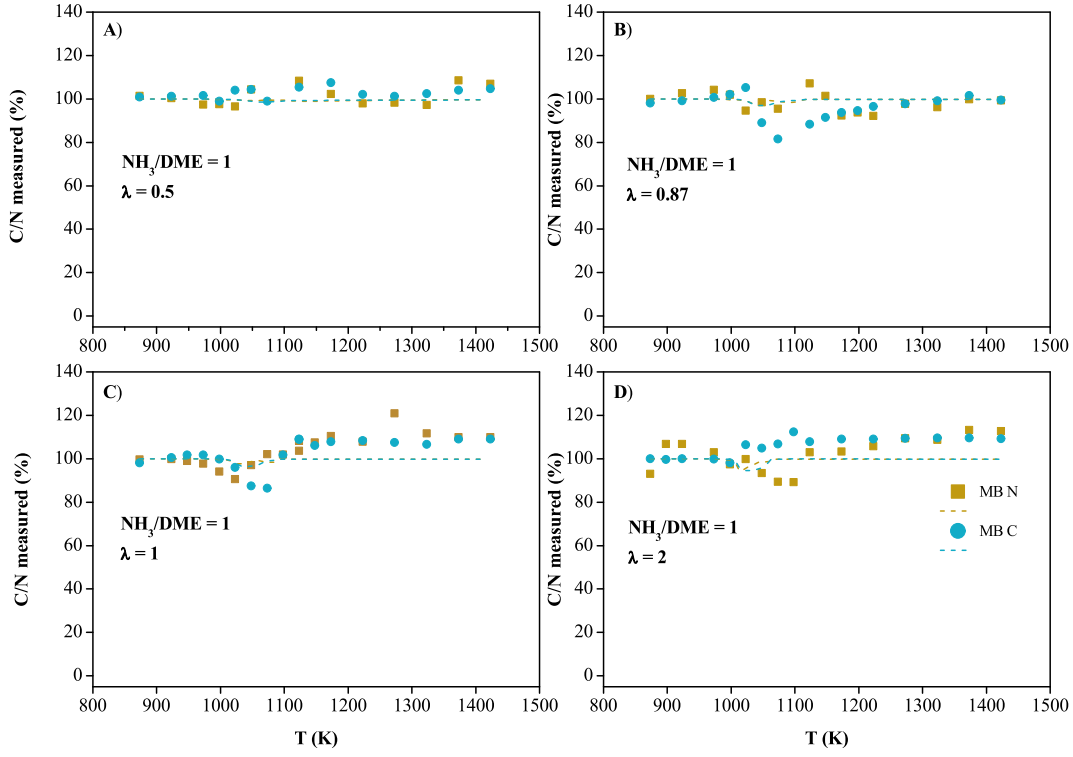

Fig. 5. Mass balance for C and N for selected experiments: A) $\lambda = 0.5$ Set 3, B) $\lambda = 0.87$ Set 4, C) $\lambda = 1$ Set 5 and D) $\lambda = 2$ Set 6.

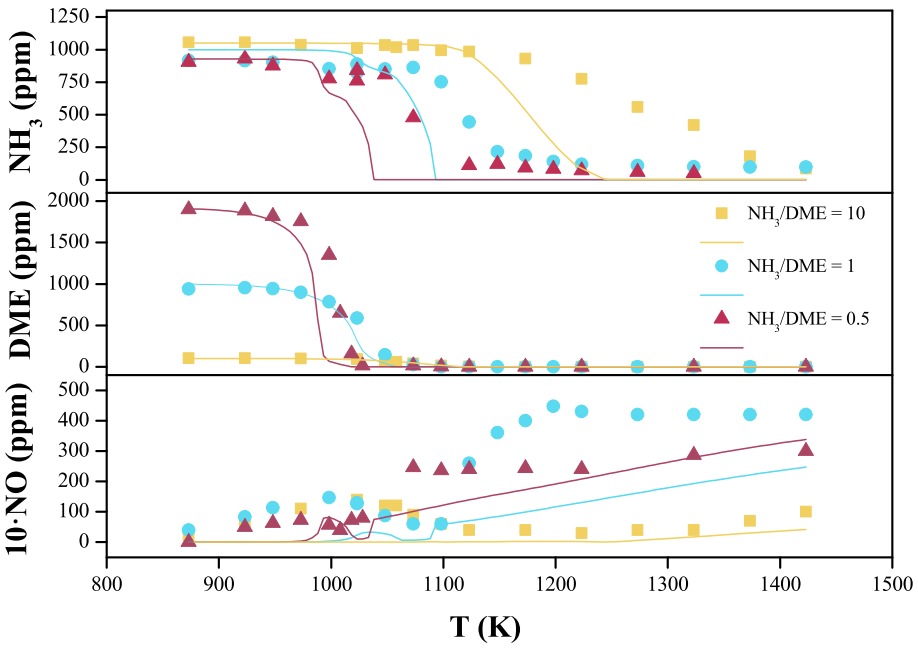

Fig. 6. NH_3, DME and NO concentrations (ppm) as a function of temperature for different NH_3/DME ratios and $\lambda \sim 1$. Sets 5, 8 and 11 of Table 1. Experimental NO concentrations are multiplied by a factor of 10.

(4) $NH_3 \rightarrow NH_2 \rightarrow H_2NO \rightarrow HNOH \rightarrow HNO \rightarrow NO \rightarrow NO_2 \rightarrow CH_3ONO$.

Reaction pathways 1 to 3 have been observed in previous studies [44,47,60]. Reaction path 4 coincides with what has been found under fuel rich conditions [41,47], forming HNO from H_2NO. As nitrogen monoxide is oxidized, NO_2 is formed, even though this happens to a small extent under the conditions of this work. NO interacts with radicals derived from the oxidation of CH_3OCH_2, producing CH_3ONO, which is thermally decomposed, generating NO again. This may explain the first NO concentration peak mentioned above, as these conditions are not favourable for the elimination of NO. Under fuel rich conditions, two new reaction pathways occur, both of which consume NO, forming N_2.

For DME and only under fuel rich conditions, there is one reaction pathway forming intermediate hydrocarbon radicals, pathway 5. This reaction pathway is not important for the other cases. The methyl radical formed produces methane in the presence of H radicals, although the calculations show a high concentration of the methyl radical as the temperature rises. Reaction pathway 5 involves the formation of formaldehyde, generating CO and CO_2, and these compounds are found in different concentrations depending on λ. There is logically a higher amount of CO_2 when $\lambda \geq 1$.

(5) $CH_3OCH_3 \rightarrow CH_3OCH_2 \rightarrow CH_2O \rightarrow CO \rightarrow CO_2$.

Other studies have also reported this reaction pathway 5 once part of the DME has been consumed [25,46,61].

Calculations indicate that there is also a reaction pathway involving the interaction of carbon radicals with NO, pathway 6. It forms CH_3ONO, which decomposes back to NO. Reaction pathway 6 involves the interaction of the CH_3O radicals, directly derived from DME, and the small amount of NO_2 present, $CH_3+NO_2 \rightleftharpoons CH_3ONO$ (−r13) to produce CH_3ONO. In turn, all the CH_3ONO formed is consumed via CH_3ONO (+M) ⇌ CH_3O+NO(+M) (−r14). This indicates that there are interactions between NH_3 and DME oxidation intermediates that are part of the NO/NO_2 chemical interconversion:

(6) $CH_3OCH_3 \rightarrow CH_3OCH_2 \rightarrow CH_3 \rightarrow CH_3ONO \rightarrow NO$. $CH_3OCH_3 \rightarrow CH_3OCH_2 \rightarrow CH_3 \rightarrow CH_3ONO \rightarrow CH_3O \rightarrow CH_2OH \rightarrow CH_2O \rightarrow HCO \rightarrow CO \rightarrow CO_2$.

We have also conducted sensitivity analyses for both NH_3, Fig. 8, and DME, Fig. 9. It is observed that the DME oxidation reactions positively affect the oxidation of NH_3. This implies that the radicals derived from DME have a significant effect on the promotion of ammonia oxidation. This is consistent with the fact that ammonia oxidation occurs at lower

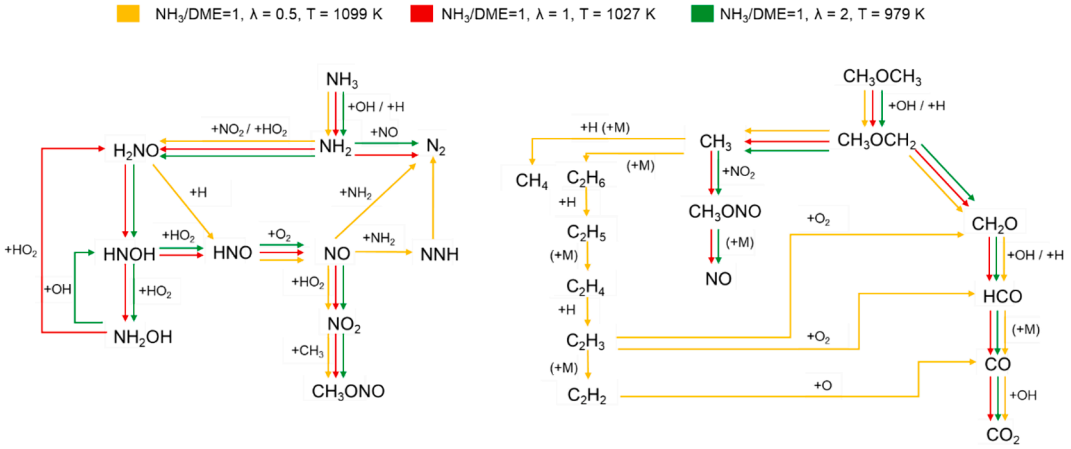

Fig. 7. Reaction pathways for NH_3 and DME conversion at different stoichiometries for NH_3/DME=1.NH_3 conversion was 10 % for each reaction pathway.

temperatures in the presence of DME. Other reactions that significantly promote ammonia consumption are those that generate OH radicals, favouring the formation of NH_2 radicals. Under fuel rich conditions, reactions $CH_3OCH_3+H \rightleftharpoons CH_3OCH_2+H_2$ (r15) and $CH_3OCH_3(+M) \rightleftharpoons CH_3OCH_2+H$ (r16) play an important role in the oxidation of DME. Those reactions mostly favour the oxidation of DME, together with $O_2+H \rightleftharpoons O+OH$ (r1), the dominant propagation reaction that generates OH and O active radicals for DME conversion [6].

Under stoichiometric and fuel lean conditions, (r17) and (r18) are the reactions that mostly dominate the oxidation of DME.

$$CH_3OCH_3(+M)+H \rightleftharpoons CH_3+CH_3O\ (+M) \quad \text{(r17)}$$

$$CH_3OCH_3+CH_3 \rightleftharpoons CH_3OCH_2+CH_4 \quad \text{(r18)}$$

Therefore, the appearance of CH_3 radicals in the radical pool also contributes to a higher oxidation of DME. At the same time, the thermal decomposition of DME, (r16) and (r17), also plays an important role in its oxidation, particularly in the first moment of the reaction, as is the case under fuel rich conditions. In terms of DME inhibition, the consumption of OH radicals by NH_3 (r2) is the most inhibiting reaction at $\lambda = 0.5$, indicating a clear competence of both ammonia and DME for OH radicals. In turn, at $\lambda \geq 1$, the reactions leading to the consumption of CH_3 radicals become more important, so the oxidation of DME by these radicals turns more relevant under these conditions.

4.2. Conversion of NH_3/DME/NO mixtures

Fig. 10 shows the comparison of the results of the two mixtures studied (without and with NO) under similar given conditions. In the presence of NO, ammonia oxidation occurs at lower temperatures (around 200 K) than in the absence of NO. In contrast, the presence of NO does not significantly affect the oxidation of DME. While the mechanism reproduces well the difference in NH_3 oxidation in the absence and presence of NO, it also predicts a difference in the DME profiles, which is not observed experimentally.

Fig. 11 plots the concentrations of NH_3, DME and NO as a function of temperature for a NH_3/DME ratio of 1 and different excess oxygen ratios. The results of the rest of the species measured are provided in Supplementary Material S7, Figures S7.1 to S7.11. Fig. 11 includes the results of two experiments conducted under similar conditions (Sets 16 and 16R of Table 1). The repeatability of these experiments is good because both show a similar behaviour at $\lambda \approx 1$.

It is shown that complete ammonia oxidation takes place at lower temperatures as the oxygen concentration increases. The mechanism reproduces fairly well the results obtained under pyrolysis and high fuel lean conditions, but does not adequately describe the specific results obtained for the stoichiometries in between, even though the main trends are captured.

The so called "NTC region" of ammonia conversion under fuel-lean conditions has been analysed at a temperature at 1050 K. The reactions most significantly contributing to ammonia inhibition were observed as $NH_2+H_2 \rightleftharpoons NH_3+H$ (−r19) and $NH_2+HO_2 \rightleftharpoons NH_3+O_2$ (2). Reaction (−19) is primarily driven by the high concentrations of H_2 present under these conditions, which makes it to proceed in the reverse sense. The presence of HO_2 radicals is attributed to the reactions $HCO+O_2 \rightleftharpoons CO+HO_2$ (r9), $CH_2OH+O_2 \rightleftharpoons CH_2O+HO_2$ (r20), and $H+O_2(+M) \rightleftharpoons HO_2(+M)$ (r21).

The formaldehyde formed in this process primarily originates from CH_2OH via the reaction $CH_2OH+O_2 \rightleftharpoons CH_2O+HO_2$ (r20). Consequently, CH_2OH plays a crucial role in promoting higher concentrations of HO_2 radicals. CH_2OH is predominantly produced through the decomposition of CH_3O via the reaction $CH_3O \rightleftharpoons CH_2OH$ (r22). The formation of CH_3O itself is associated with the presence of nitrogenous compounds, specifically through the reaction $CH_3ONO(+M) \rightleftharpoons CH_3O+NO(+M)$ (r14).

Additionally, CH_3ONO is formed only from the reaction $CH_3+NO_2 \rightleftharpoons CH_3ONO$ (r13). The methyl radicals in reaction (r13) are derived from the decomposition of CH_3OCH_2 and the interaction of CH_4 with OH radicals, as described by $CH_4+OH \rightleftharpoons CH_3+H_2O$ (r23). Methane, in turn, is produced through reactions involving CH_3 radicals, such as $CH_3+H(+M) \rightleftharpoons CH_4(+M)$ (r24) and $CH_3+HO_2 \rightleftharpoons CH_4+O_2$ (r25). Thus, the decomposition pathway of CH_3OCH_2 plays a fundamental role for all the above-mentioned interactions to take place.

Compared to stoichiometric conditions, DME oxidation occurs at lower temperatures (100 K) under fuel lean conditions, coinciding with the reported results for DME conversion in the presence of NO [52]. However, the NO reduction obtained with NH_3 and DME together is smaller than that of the DME-NO mixtures, around 80 % [52]. When NH_3 is present in the mixture, the maximum NO reductions are around 60 %. NO reductions are observed for $\lambda = 1$ and above. The most important reductions occur at $\lambda = 2$, so the initial O_2 concentration highly influences the NO reductions achieved. This behaviour has been seen in other studies that use the NH_3/NO mixture [49,62], which

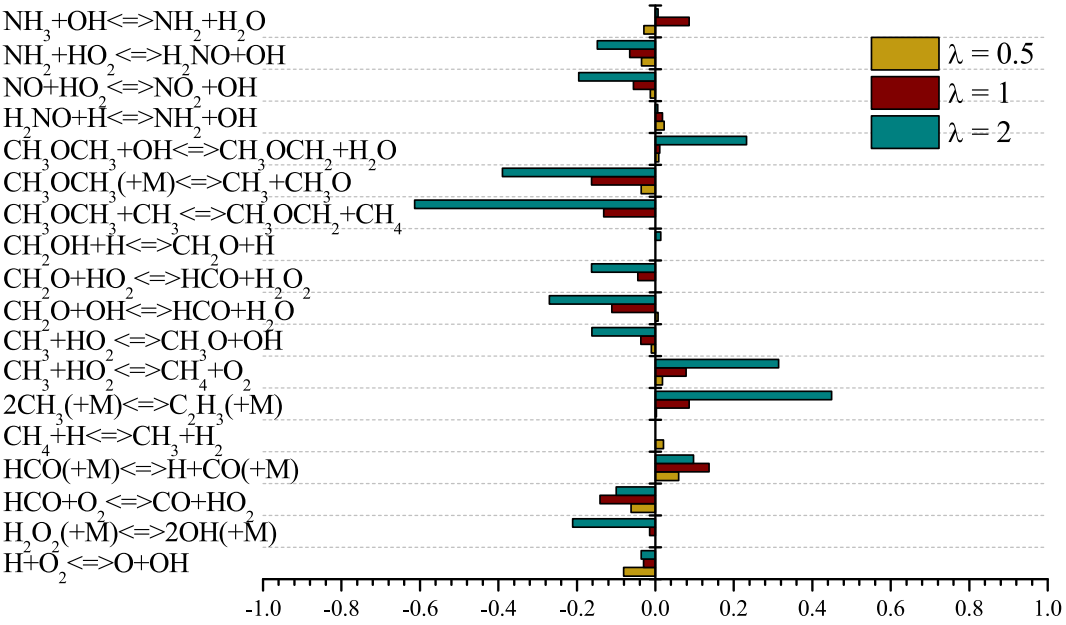

Fig. 8. Sensitivity study of NH_3 consumption at different λ and for a NH_3/DME ratio of 1 when 10 % of NH_3 is consumed.

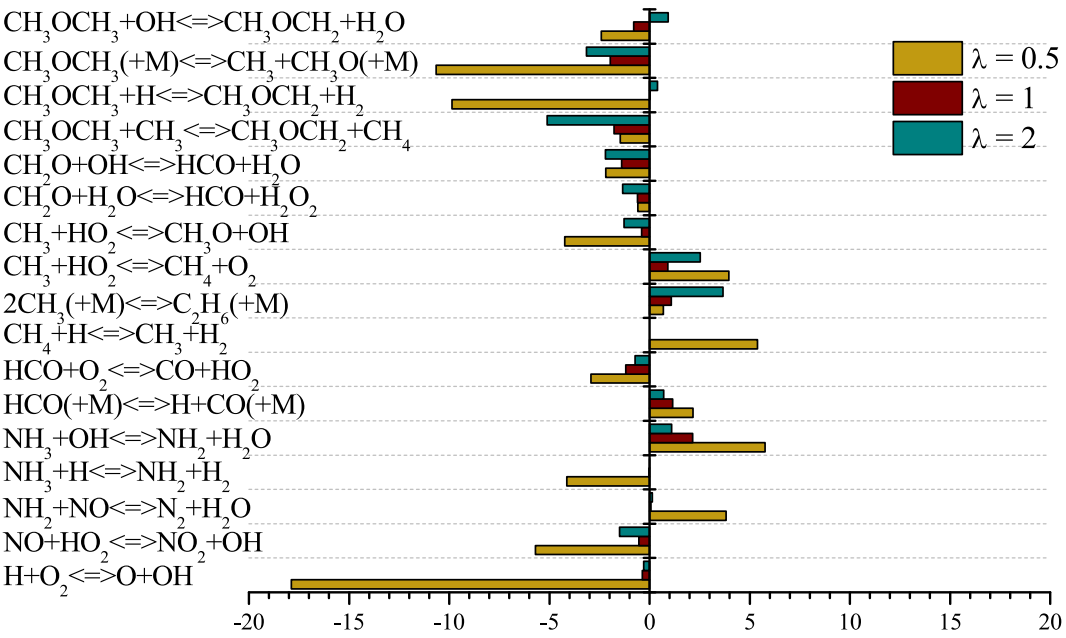

Fig. 9. Sensitivity study of DME consumption at different λ and for a NH_3/DME ratio of 1 when 10 % of NH_3 is consumed.

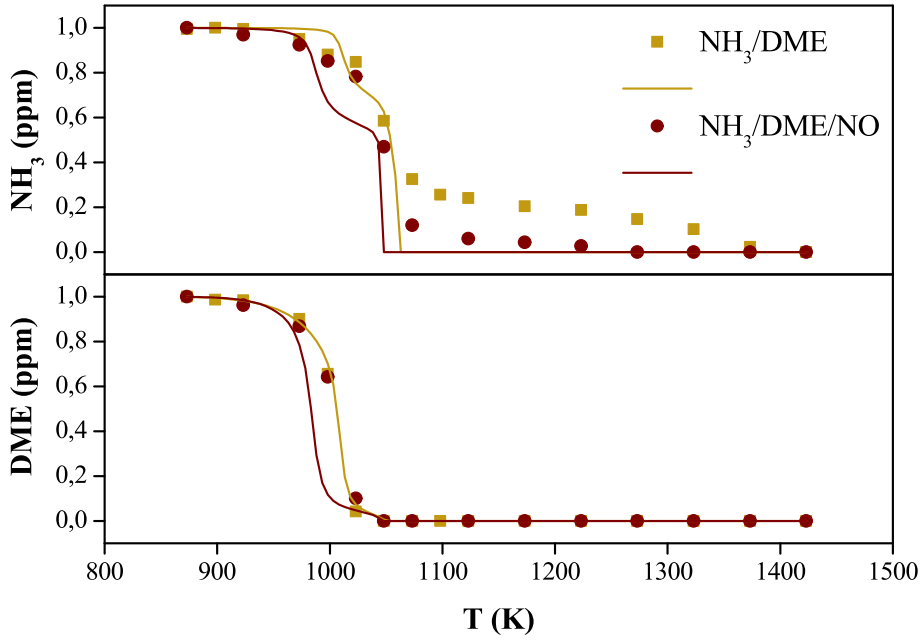

Fig. 10. Results of NH_3 and DME both in the absence and presence of approximately 1000 ppm NO as a function of temperature, at λ ≈ 1 and NH_3/DME ≈ 1. Sets 5 and 16 of Table 1.

indicates the significance of the SNCR reaction mechanism under the present conditions.

In the presence of NO, the addition of a higher concentration of DME has the same effect as that seen in the absence of NO. The complete oxidation of DME between a NH_3/DME of 10 and 0.5 occurs with a difference of 75 K, so the change is small in the presence of NO. However, for ammonia, the results obtained are similar to those achieved in the absence of NO, with temperature differences of 175 K when 150 ppm of NH_3 remain at the reactor outlet.

Changes in the NH_3/DME ratio affect NO reductions. A difference of around 175 K is observed between the different minimum NO concentrations measured in Sets 16, 19 and 22 (λ ≈ 1 and different NH_3/DME ratios). The corresponding results can be found in the Supplementary Material S8, Figures S8.1 to S8.14.

Regarding the variation of λ with different NH_3/DME mixture ratios, the behaviour is similar to the previous one shown in Fig. 6. A higher ammonia conversion is obtained at lower temperatures when the proportion of DME increases. In the same way, the maximum NO reductions also occur under the most oxidizing conditions. No variations are found in the oxidation of DME, and its complete conversion is observed at approximately 1125 K.

For the NH_3/DME/NO mixture, a kinetic study has also been carried out, based on the reaction paths of the added fuels (Fig. 12) and the sensitivity analyses of both NH_3 and DME (Figs. 13 and 14 respectively).

There are several differences compared to what happens in the absence of NO, Fig. 7. The presence of NO (≈1000 ppm) leads to a

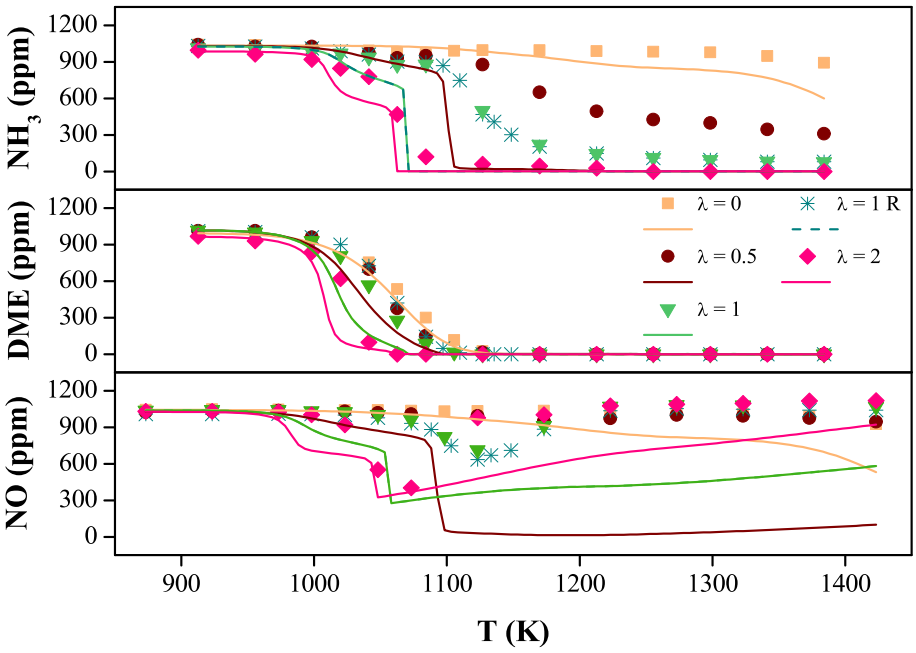

Fig. 11. NH_3, DME and NO concentrations as a function of temperature for different stoichiometries. Sets 13, 15, 16, 16R and 17 of Table 1.

predominance of NH_2 reacting with NO, with nitrogen produced by two different reaction pathways:

(7) $NH_3 \rightarrow NH_2 \rightarrow NNH \rightarrow N_2$.

(8) $NH_3 \rightarrow NH_2 \rightarrow N_2$.

In the presence of NO, the oxidation of NH_3 at the onset of the reaction is exclusively due to its interaction with NO. Reaction $NO+HO_2 \rightleftharpoons NO_2+OH$ (r11) is important for $\lambda = 1$ and NH_3/DME=1 and responsible for the increase in OH radicals, which favour the oxidation of NH_3 when NO is present. As mentioned above, NO_2 is consumed in the reaction $CH_3+NO_2 \rightleftharpoons CH_3ONO$ (r13). Calculations indicate that this reaction takes place to a considerable extent. This differs from what happens in the mixtures without NO, with a clear and significant formation of NO from the oxidation of NH_2 radicals. This occurs only in the section where there is a decrease in NO concentrations (the temperature range changes depending on the O_2 concentrations in the mixture).

This CH_3 and NO reaction adds complexity to the DME reaction pathways, as four options have been found:

(6) $CH_3OCH_3 \rightarrow CH_3OCH_2 \rightarrow CH_3 \rightarrow CH_3ONO \rightarrow NO$

$CH_3OCH_3 \rightarrow CH_3OCH_2 \rightarrow CH_3 \rightarrow CH_3ONO \rightarrow CH_3O \rightarrow CH_2OH \rightarrow CH_2O \rightarrow HCO \rightarrow CO \rightarrow CO_2$.

(9) $CH_3OCH_3 \rightarrow CH_3OCH_2 \rightarrow CH_2O \rightarrow HCO \rightarrow CO \rightarrow CO_2$.

(10) $CH_3OCH_3 \rightarrow CH_3OCH_2 \rightarrow CH_2O \rightarrow HCO \rightarrow HNO \rightarrow NO$.

(11) $CH_3OCH_3 \rightarrow CH_3OCH_2 \rightarrow CH_3 \rightarrow CH_3ONO \rightarrow CH_3O \rightarrow CH_2OH \rightarrow CH_2O \rightarrow HCO \rightarrow HNO \rightarrow NO$.

The first two pathways (6 and 9) end in the formation of CO/CO_2. Pathway 6 is the same as that presented in the NO-free mixtures. When there is no excess oxygen, additional reaction pathways (10 and 11) become important. These pathways may explain why it is not possible to achieve greater NO reductions under fuel rich conditions. In addition, the non-occurrence of pathways (10–11) for $\lambda = 2$ indicates why more

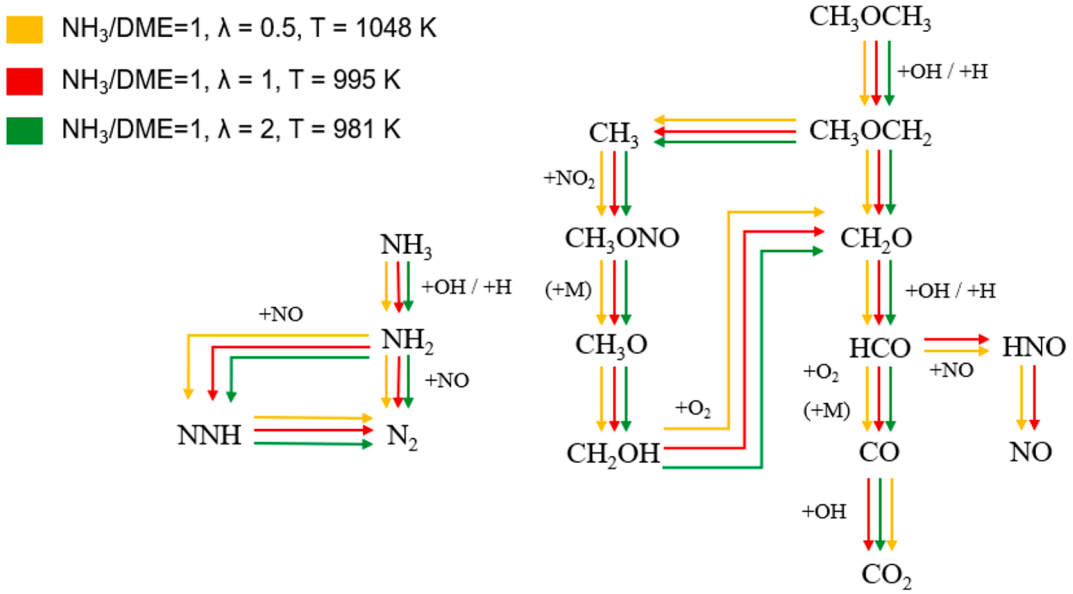

Fig. 12. Reaction pathways for NH_3 and DME at different stoichiometries for NH_3/DME/NO=1.NH_3 conversion was 10 %.

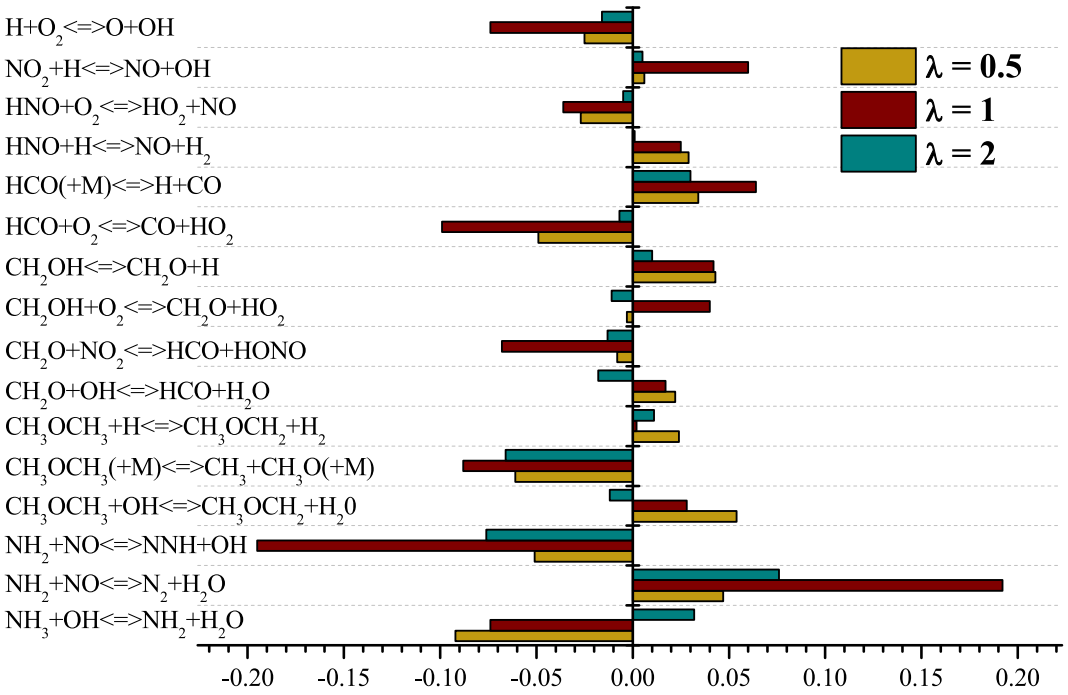

Fig. 13. Sensitivity study of NH_3 at different λ for NH_3/DME/NO=1.NH_3 conversion was 10 %.

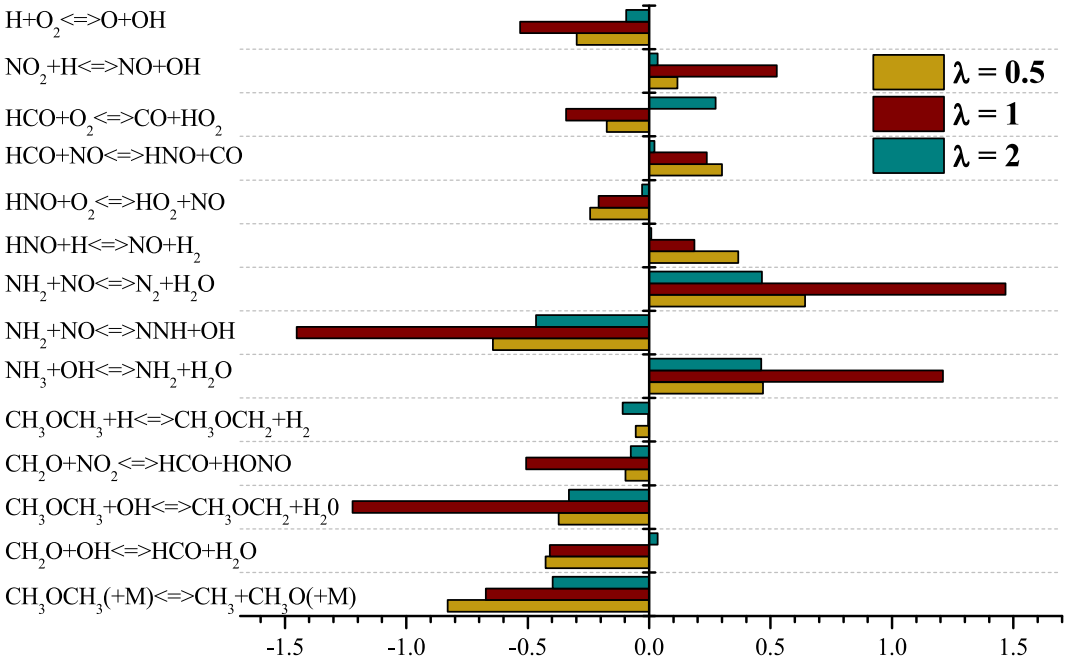

Fig. 14. Sensitivity study of DME at different λ for NH_3/DME/NO=1.NH_3 conversion was 10 %.

NO is consumed, inhibiting two of the reactions that would increase the NO concentration. However, NO is still formed from the decomposition reactions CH_3ONO (+M)⇌CH_3O+NO(+M) (r14) and HNO(+M)⇌NO+H(+M) (r26). It is worth noting that no significant reburn interactions are identified under the conditions studied.

Sensitivity analyses were carried out at temperatures at which 10 % of the NH_3 was consumed. The temperatures for the sensitivity analysis are the same as those for the reaction pathways in Fig. 12. According to the sensitivity analysis, Figs. 13 and 14, there are some reactions that markedly affect ammonia oxidation for any of the conditions presented in the study. Reactions NH_2+NO⇌N_2+H_2O (r3) and CH_3OCH_3(+M)⇌CH_3+CH_3O(+M) (r27) are among those that have the most positive effect on NH_3 oxidation for the three λ studied, together with (r1): O_2+H⇌O+OH, which is known to have a strong effect on the radical pool.

Reactions of NH_3 and derivatives together with the radical pool, especially the OH radical, play an important role in the initiation of ammonia oxidation. It is observed that the most important reaction in NH_3 consumption is NH_2+NO⇌N_2+H_2O (r3), which predominates once NH_2 has been formed from NH_3. The main reaction pathway from ammonia oxidation to N_2 is found to be NH_3 → NH_2 → N_2 (7). This is due to the fact that even though the other simultaneous reaction pathway,

$NH_3 \rightarrow NH_2 \rightarrow NNH \rightarrow N_2$ (8), shows the most inhibitory effect on NH_3 oxidation under all λ conditions, it is not the fastest, and therefore, not the main one. Although $NH_2+NO \rightleftharpoons N_2+H_2O$ (r3) is the faster of the two proposed reactions between NH_2 and NO, it is also the one that causes a higher consumption of NO, which is the main reason for the lower temperature consumption of NH_3. This has a global inhibitory effect on NH_3 oxidation since NH_3. $NH_2+NO \rightleftharpoons NNH+OH$ (r4) is an important chain branching reaction leading to the formation of OH radicals. Therefore, the fact that (r3) is the dominant reaction under the present specific conditions implies somehow that there is an inhibition of the NH_3 oxidation process.

Under the conditions in which the sensitivity analysis for NH_3 has been carried out, there are reactions from DME that become important to increase NH_3 oxidation. $CH_3OCH_3(+M) \rightleftharpoons CH_3+CH_3O(+M)$ (r27) will always stimulate the oxidation of NH_3, as it contributes to the radical pool. In the case of $CH_3OCH_3+OH \rightleftharpoons CH_3OCH_2+H_2O$ (r28), it will only favour NH_3 consumption in cases with excess oxygen, as there will be plenty of OH for both fuels. However, under fuel lean and stoichiometric conditions, both fuels compete for OH radicals, with (r28) restricting NH_3 oxidation.

Regarding DME, it is found that the reaction path of ammonia conversion occurring through NNH is positive for DME conversion. This is because NNH decomposes into N_2 without the need to consume more OH radicals. As mentioned above, OH and the radicals formed in the decomposition reaction of DME are the most important reactions for the formation of CH_3OCH_2. (r1) chain branching reaction is again important because it increases the concentration of OH and O radicals. The most unfavourable reactions for the conversion of DME at any λ are those where NH_3 is converted into NH_2 radicals, (r2) and (r4). This is due to the high consumption of radicals that these reactions involve. This is again an indication of the competition between both fuels (DME and NH_3) for the radical pool constituents.

5. Conclusions

Oxidation experiments on NH_3/DME and NH_3/DME/NO mixtures have been carried out for different O_2 (λ) conditions and NH_3/DME ratios in a temperature range of 875–1425 K, and the results have been interpreted in terms of a chemical kinetic mechanism detailed in the literature. The ultimate goal of these experiments and subsequent simulations is to increase the experimental database of the mentioned mixtures and to evaluate the impact of NO on NH_3/DME mixtures.

The presence of DME in the NH_3/DME mixture shifts the temperature at which NH_3 is oxidized, especially under fuel lean conditions and as the DME concentration increases. This is due to the fact that DME is the main compound in the mixture, which results in lower ignition temperatures that are increasingly similar to those of pure DME. The increase of oxygen in the medium does not strongly influence the oxidation temperatures of DME. NO production occurs at low concentrations (81 ppm maximum) during the NH_3/DME oxidation experiments. This indicates that the addition of DME produces a decrease in NO that is not found in pure NH_3 combustion. While NO reduction by reburn reactions does not seem to be significant, the reduction of NO in the presence of DME is attributed to SNCR reactions and possibly also to the interaction between DME and NH_3, or their derivatives.

The experimentally measured compounds efficiently cover the behaviour of the studied mixture, as shown from the C and N balances, even though it would be good to properly determine CH_2O.

Both NH_3 and DME compete at times for OH radicals in the presence and absence of NO. This is because in the initial stages of the reaction both reactants have a significant dependence on OH radicals for oxidation.

With the addition of NO, the temperature at which NH_3 is oxidised is lower in all the mixture conversion cases. This does not occur with DME, where noticeable differences are only seen under fuel lean conditions. In addition, reductions of up to 61 % in NO concentrations are obtained in the NH_3/DME mixture. These reductions increase under fuel lean conditions, although more important reductions are achieved in mixtures with net ammonia, i.e. in the absence of DME.

The addition of NO highly affects the oxidation of NH_3, which follows completely different reaction pathways than those observed for the NH_3/DME mixture. In the case of DME, its reaction pathways are influenced only by certain secondary ones.

Concerning the calculations, at NH_3/DME=1, the model describes, in general, the main trends experimentally observed. However, there is still room for improvement in relation to the specific concentration values. The highest differences between experimental and calculated results are found under those conditions where the NH_3/DME ratio is different from 1. Therefore, further study and development of the model is still desirable.

CRediT authorship contribution statement

A. Ruiz-Gutiérrez: Writing – original draft, Resources, Methodology, Formal analysis, Data curation. **P. Rebollo:** Methodology, Data curation. **M.U. Alzueta:** Writing – review & editing, Supervision, Conceptualization, Funding acquisition.

Declaration of competing interest

The authors declare that they have no known competing financial interests or personal relationships that could have appeared to influence the work reported in this paper.

Data availability

Data will be made available on request.

Acknowledgments

The authors express their gratitude to grant PID2021-12432OB-I00 and TED2021-129557B-I00, funded by MCIN/AEI/10.13039/501100011033 and "ERDF A way of making Europe", by the "European Union" and to Aragón Government (Ref. T22_23R) and to the predoctoral grant awarded to Mr. Ruiz-Gutiérrez, PRE2022-104181 grant funded by MICIN.

Appendix A. Supplementary material

Supplementary data to this article can be found online at https://doi.org/10.1016/j.fuel.2024.133253.

References

[1] World Energy Statistics and Balances - Data product - IEA https://www.iea.org/data-and-statistics/data-product/world-energy-statistics-and-balances (accessed April 25, 2024).
[2] Understanding Global Warming Potentials | US EPA https://www.epa.gov/ghgemissions/understanding-global-warmingpotentials (accessed April 25, 2024).
[3] Energy Agency I. Net Zero by 2050 - A Roadmap for the Global Energy Sector. 2050. https://www.iea.org/reports/net-zero-by-2050 (accessed April 29, 2024).
[4] Campion N, Nami H, Swisher PR, Vang Hendriksen P, Münster M. Techno-economic assessment of green ammonia production with different wind and solar potentials. Renewable Sustainable Energy Rev 2023;173:113057. https://doi.org/10.1016/j.rser.2022.113057.
[5] Kojima Y, Liquid ammonia for hydrogen storage – Hiroshima University. https://nh3fuel.wordpress.com/wp-content/uploads/2014/10/nh3fa-2014-yoshitsugu-kojima.pdf (accessed April 29, 2024).
[6] Zhu S, Xu Q, Tang R, Gao J, Wang Z, Pan J, et al. A comparative study of oxidation of pure ammonia and ammonia/dimethyl ether mixtures in a jet-stirred reactor using SVUV-PIMS. Combust Flame 2023;250:112643. https://doi.org/10.1016/j.combustflame.2023.112643.
[7] Dincer I, Midilli A, Hepbasli A, Hikmet-Karakoc T. Global warming: Engineering solutions. London: Publishing Inc Springer; 2010. p. 110.
[8] Okafor EC, Somarathne KDKA, Hayakawa A, Kudo T, Kurata O, Iki N, et al. Towards the development of an efficient low-NO_x ammonia combustor for a micro

gas turbine. Proc Combust Inst 2019;37:4597–606. https://doi.org/10.1016/j.proci.2018.07.083.
[9] Test Results of the Ammonia Mixed Combustion at Mizushima Power Station Unit No.2 and Related Patent Applications – Ammonia Energy Association https://www.ammoniaenergy.org/paper/test-results-of-the-ammonia-mixed-combustion-at-mizushima-power-station-unit-no-2-and-related-patent-applications/ (accessed April 8, 2024).
[10] Cardoso JS, Silva V, Rocha RC, Hall MJ, Costa M, Eusébio D. Ammonia as an energy vector: Current and future prospects for low-carbon fuel applications in internal combustion engines. J Clean Prod 2021;296:126562. https://doi.org/10.1016/j.jclepro.2021.126562.
[11] Haputhanthri SO, Maxwell TT, Fleming J, Austin C. Ammonia and gasoline fuel blends for spark ignited internal combustion engines. J Energy Resour Technol 2015;137:062201. https://doi.org/10.1115/1.4030443.
[12] Okanishi T, Okura K, Srifa A, Muroyama H, Matsui T, Kishimoto M, et al. Comparative study of ammonia-fueled solid oxide fuel cell systems. Fuel Cells 2017;17:383–90. https://doi.org/10.1002/fuce.201600165.
[13] Hayakawa A, Goto T, Mimoto R, Kudo T, Kobayashi H. NO formation/reduction mechanisms of ammonia/air premixed flames at various equivalence ratios and pressures. Mech Eng J 2015;2:14–00402. https://doi.org/10.1299/mej.14-00402.
[14] Dai L, Gersen S, Glarborg P, Mokhov A, Levinsky H. Autoignition studies of NH_3/CH_4 mixtures at high pressure. Combust Flame 2020;218:19–26. https://doi.org/10.1016/j.combustflame.2020.04.020.
[15] Xiao H, Lai S, Valera-Medina A, Li J, Liu J, Fu H. Study on counterflow premixed flames using high concentration ammonia mixed with methane. Fuel 2020;275:117902. https://doi.org/10.1016/j.fuel.2020.117902.
[16] García-Ruiz P, Salas I, Casanova E, Bilbao R, Alzueta MU. Experimental and Modeling High-Pressure Study of Ammonia-Methane Oxidation in a Flow Reactor. Energy Fuels 2024;38:1399–415. https://doi.org/10.1021/acs.energyfuels.3c03959.
[17] Mei B, Zhang J, Shi X, Xi Z, Li Y. Enhancement of ammonia combustion with partial fuel cracking strategy: Laminar flame propagation and kinetic modeling investigation of NH_3/H_2/N_2/air mixtures up to 10 atm. Combust Flame 2021;231:111472. https://doi.org/10.1016/j.combustflame.2021.111472.
[18] Ichikawa A, Hayakawa A, Kitagawa Y, Kunkuma Amila Somarathne KD, Kudo T, Kobayashi H. Laminar burning velocity and Markstein length of ammonia/hydrogen/air premixed flames at elevated pressures. Int J Hydrogen Energy 2015;40:9570–8. https://doi.org/10.1016/j.ijhydene.2015.04.024.
[19] Lee JH, Lee SI, Kwon OC. Effects of ammonia substitution on hydrogen/air flame propagation and emissions. Int J Hydrogen Energy 2010;35:11332–41. https://doi.org/10.1016/j.ijhydene.2010.07.104.
[20] Lhuillier C, Brequigny P, Lamoureux N, Contino F, Mounaïm-Rousselle C. Experimental investigation on laminar burning velocities of ammonia/hydrogen/air mixtures at elevated temperatures. Fuel 2020;263:116653. https://doi.org/10.1016/j.fuel.2019.116653.
[21] Alzueta MU, Mercader V, Cuoci A, Gersen S, Hashemi H, Glarborg P. Flow reactor oxidation of ammonia-hydrogen fuel mixtures. Energy Fuels 2024;38:3369–81. https://doi.org/10.1021/acs.energyfuels.3c03929.
[22] García-Ruiz P, Castejón D, Abengoechea M, Bilbao R, Alzueta MU. High-pressure study of the conversion of NH_3/H_2 mixtures in a flow reactor. 40th International Symposium on Combustion, Milano (Italy), July 2024 (accepted for presentation).
[23] Marrodán L, Millera Á, Bilbao R, Alzueta MU. An experimental and modeling study of acetylene-dimethyl ether mixtures oxidation at high-pressure. Fuel 2022;327:125143. https://doi.org/10.1016/j.fuel.2022.125143.
[24] Marrodán L, Millera Á, Bilbao R, Alzueta MU. Experimental and modeling evaluation of dimethoxymethane as an additive for high-pressure acetylene oxidation. J Phys Chem A 2022;126:6253–63. https://doi.org/10.1021/acs.jpca.2c03130.
[25] Xiao H, Li H. Experimental and kinetic modeling study of the laminar burning velocity of NH_3/DME/air premixed flames. Combust Flame 2022;245:112372. https://doi.org/10.1016/j.combustflame.2022.112372.
[26] Gross CW, Kong SC. Performance characteristics of a compression-ignition engine using direct-injection ammonia-DME mixtures. Fuel 2013;103:1069–79. https://doi.org/10.1016/j.fuel.2012.08.026.
[27] Shi X, Li W, Zhang J, Fang Q, Zhang Y, Xi Z, et al. Exploration of NH_3 and NH_3/DME laminar flame propagation in O_2/CO_2 atmosphere: Insights into NH_3/CO_2 interactions. Combust Flame 2024;260:113245. https://doi.org/10.1016/j.combustflame.2023.113245.
[28] Issayev G, Giri BR, Elbaz AM, Shrestha KP, Mauss F, Roberts WL, et al. Combustion behavior of ammonia blended with diethyl ether. Proc Combust Inst 2021;38:499–506. https://doi.org/10.1016/j.proci.2020.06.337.
[29] Sakai Y, Herzler J, Werler M, Schulz C, Fikri M. A quantum chemical and kinetics modeling study on the autoignition mechanism of diethyl ether. Proc Combust Inst 2017;36:195–202. https://doi.org/10.1016/j.proci.2016.06.037.
[30] Shrestha KP, Giri BR, Elbaz AM, Issayev G, Roberts WL, Seidel L, et al. A detailed chemical insight into the kinetics of diethyl ether enhancing ammonia combustion and the importance of NO_x recycling mechanism. Fuel 2022;10:100051. https://doi.org/10.1016/j.jfueco.2022.100051.
[31] Elbaz AM, Giri BR, Issayev G, Shrestha KP, Mauss F, Farooq A, et al. Experimental and kinetic modeling study of laminar flame speed of dimethoxymethane and ammonia blends. Energy Fuels 2020;34:14726–40. https://doi.org/10.1021/acs.energyfuels.0c02269.
[32] Shahpouri S, Norouzi A, Hayduk C, Fandakov A, Rezaei R, Koch CR, et al. Laminar flame speed modeling of hydrogen, methanol and ammonia using machine learning of machine learning. Congress: Canadian Soc. for Mechanical Eng. Int; 2022.
[33] Burke U, Metcalfe WK, Burke SM, Heufer KA, Dagaut P, Curran HJ. A detailed chemical kinetic modeling, ignition delay time and jet-stirred reactor study of methanol oxidation. Combust Flame 2016;165:125–36. https://doi.org/10.1016/j.combustflame.2015.11.004.
[34] DME Handbook,Japan DME Forum,2001.
[35] Ereña J, Sierra I, Aguayo AT, Ateka A, Olazar M, Bilbao J. Kinetic modelling of dimethyl ether synthesis from (H_2+CO_2) by considering catalyst deactivation. Chem Eng J 2011;174:660–7. https://doi.org/10.1016/j.cej.2011.09.067.
[36] Peláez R, Marín P, Ordóñez S. Direct synthesis of dimethyl ether from syngas over mechanical mixtures of CuO/ZnO/Al_2O_3 and Γ-Al_2O_3: Process optimization and kinetic modelling. Fuel Process Technol 2017;168:40–9. https://doi.org/10.1016/j.fuproc.2017.09.004.
[37] Park SH, Lee CS. Combustion performance and emission reduction characteristics of automotive DME engine system. Prog Energy Combust Sci 2013;39:147–68. https://doi.org/10.1016/j.pecs.2012.10.002.
[38] Pelucchi M, Schmitt S, Gaiser N, Cuoci A, Frassoldati A, Zhang H, et al. On the influence of NO addition to dimethyl ether oxidation in a flow reactor. Combust Flame 2022;257:112464. https://doi.org/10.1016/j.combustflame.2022.112464.
[39] Bae C, Kim J. Alternative fuels for internal combustion engines. Proc Combust Inst 2017;36:3389–413. https://doi.org/10.1016/j.proci.2016.09.009.
[40] Lee S, Oh S, Choi Y, Kang K. Performance and emission characteristics of a CI engine operated with n-Butane blended DME fuel. Appl Therm Eng 2011;31:1929–35. https://doi.org/10.1016/j.applthermaleng.2011.02.039.
[41] Yin G, Xiao B, Zhao H, Zhan H, Hu E, Huang Z. Jet-stirred reactor measurements and chemical kinetic study of ammonia with dimethyl ether. Fuel 2023;341:127542. https://doi.org/10.1016/j.fuel.2023.127542.
[42] Dagaut P. On the Oxidation of Ammonia and Mutual Sensitization of the Oxidation of NO and Ammonia: Experimental and Kinetic Modeling. Combust Sci Technol 2022;194:117–29. https://doi.org/10.1080/00102202.2019.1678380.
[43] Meng X, Zhang M, Zhao C, Tian H, Tian J, Long W, et al. Study of combustion and NO chemical reaction mechanism in ammonia blended with DME. Fuel 2022;319:123832. https://doi.org/10.1016/j.fuel.2022.123832.
[44] Cai T, Zhao D. Enhancing and assessing ammonia-air combustion performance by blending with dimethyl ether. Renewable Sustainable Energy Rev 2022;156:112003. https://doi.org/10.1016/j.rser.2021.112003.
[45] Issayev G, Giri BR, Elbaz AM, Shrestha KP, Mauss F, Roberts WL, et al. Ignition delay time and laminar flame speed measurements of ammonia blended with dimethyl ether: A promising low carbon fuel blend. Renew Energy 2022;181:1353–70. https://doi.org/10.1016/j.renene.2021.09.117.
[46] Dai L, Hashemi H, Glarborg P, Gersen S, Marshall P, Mokhov A, et al. Ignition delay times of NH_3 /DME blends at high pressure and low DME fraction: RCM experiments and simulations. Combust Flame 2021;227:120–34. https://doi.org/10.1016/j.combustflame.2020.12.048.
[47] Murakami Y, Nakamura H, Tezuka T, Hiraoka K, Maruta K. Effects of mixture composition on oxidation and reactivity of DME/NH_3/air mixtures examined by a micro flow reactor with a controlled temperature profile. Combust Flame 2022;238:111911. https://doi.org/10.1016/j.combustflame.2021.111911.
[48] Han X, Wang Z, Costa M, Sun Z, He Y, Cen K. Experimental and kinetic modeling study of laminar burning velocities of NH_3/air, NH_3/H_2/air, NH_3/CO/air and NH_3/CH_4/air premixed flames. Combust Flame 2019;206:214–26. https://doi.org/10.1016/j.combustflame.2019.05.003.
[49] Alzueta MU, Ara L, Mercader VD, Delogu M, Bilbao R. Interaction of NH_3 and NO under combustion conditions. Experimental flow reactor study and kinetic modeling simulation. Combust Flame 2022; 235: 111691. DOI: 10.1016/j.combustflame.2021.111691.
[50] Kasuya F, Glarborg P, Johnsson JE, Dam-Johansen K. The thermal DeNOx process: Influence of partial pressures and temperature. Chem Eng Sci 1995;50:1455–66. https://doi.org/10.1016/0009-2509(95)00008-S.
[51] Rota R, Verton ED, Zanoelo F, Antos D, Morbidelli M, Carrà S. Analysis of the thermal $DeNO_x$ process at high partial pressure of reactants. Chem Eng Sci 2000;55:1041–51. https://doi.org/10.1016/S0009-2509(99)00011-1.
[52] Alzueta MU, Muro J, Bilbao R, Glarborg P. Oxidation of dimethyl ether and its interaction with nitrogen oxides. Isr J Chem 1999;39:73–86. https://doi.org/10.1002/ijch.199900008.
[53] Hashemi H, Christensen JM, Glarborg P. High-pressure pyrolysis and oxidation of DME and DME/CH_4. Combust Flame 2019;205:80–92. https://doi.org/10.1016/j.combustflame.2019.03.028.
[54] Alzueta MU, Pernía R, Abián M, Millera Á, Bilbao R. CH_3SH conversion in a tubular flow reactor. Experiments and kinetic modelling Combust Flame 2019;203:23–30. https://doi.org/10.1016/j.combustflame.2019.01.017.
[55] Glarborg P, Miller JA, Ruscic B, Klippenstein SJ. Modeling nitrogen chemistry in combustion. Prog Energy Combust Sci 2018;67:31–68. https://doi.org/10.1016/j.pecs.2018.01.002.
[56] Abián M, Benés M, de Goñi A, Muñoz B, Alzueta MU. Study of the oxidation of ammonia in a flow reactor. Experiments and kinetic modeling simulation Fuel 2021;300:120979. https://doi.org/10.1016/j.fuel.2021.120979.
[57] Alzueta MU, Guerrero M, Millera Á, Marshall P, Glarborg P. Experimental and kinetic modeling study of oxidation of acetonitrile. Proc Combust Inst 2021;38:575–83. https://doi.org/10.1016/j.proci.2020.07.043.
[58] Alzueta MU, Abián M, Elvira I, Mercader VD, Sieso L. Unraveling the NO reduction mechanisms occurring during the combustion of NH_3/CH_4 mixtures. Combust Flame 2022. 2023; 257: 112531 DOI: 10.1016/j.combustflame.2022.112531.
[59] Ansys CHEMKIN-PRO 2023 R1. Ansys Inc., 2023.

[60] Cai T, Zhao D. Temperature dependence of laminar burning velocity in ammonia/dimethyl ether-air premixed flames. J Therm Sci 2022;31:189–97. https://doi.org/10.1007/s11630-022-1549-1.
[61] Yin G, Li J, Zhou M, Li J, Wang C, Hu E, et al. Experimental and kinetic study on laminar flame speeds of ammonia/dimethyl ether/air under high temperature and elevated pressure. Combust Flame 2022;238:111915. https://doi.org/10.1016/j.combustflame.2021.111915.
[62] Feng G, Chen J, Fan W, Wang X. Study of the interaction between NH_3 and NO in the reduction zone of air-staged ammonia combustion under high moisture atmosphere. J Clean Prod 2023;409:137218. https://doi.org/10.1016/j.jclepro.2023.137218.